Russian Geology and Geophysics © 2020, V.S. Sobolev IGM, Siberian Branch of the RAS
Vol. 61, No. 1, pp. 36–46, 2020 *DOI:10.15372/RGG2019076* *Geologiya i Geofizika*

Minerals of the System Stichtite–Pyroaurite–Iowaite–Woodallite from Serpentinites of the Terekta Ridge (Gorny Altai, Russia)

E.S. Zhitova[a, ✉], I.V. Pekov[b], N.V. Chukanov[b,c], V.O. Yapaskurt[b], V.N. Bocharov[a]

[a]*St. Petersburg University, Universitetskaya nab. 7/9, St. Petersburg, 199034 Russia*

[b]*Lomonosov Moscow State University, Leninskie Gory GSP-1, Moscow, 119991, Russia*

[c]*Institute of Problems of Chemical Physics of RAS, pr. Akademika Semenova 1, Chernogolovka, 142432, Russia*

Received 26 April 2018; accepted 17 September 2018

Abstract—Hydrotalcite supergroup minerals stichtite, pyroaurite, iowaite, and woodallite form a complex solid-solution system at the Kyzyl-Uyuk locality (Terekta Ridge, Gorny Altai, Russia). The diversity of these minerals is due to: (1) subdivision by anionic interlayer composition into carbonate (stichtite and pyroaurite) and chloride (iowaite and woodallite) species and (2) isomorphism of M^{3+} cations, mainly between Cr- (stichtite and woodallite) and Fe^{3+}-dominant species (pyroaurite and iowaite), with a quantitative predominance of stichtite and iowaite. Most of the studied samples correspond to stichtite and woodallite with high Fe^{3+} contents or pyroaurite and iowaite with high Cr^{3+} contents. According to vibrational (IR and Raman) spectroscopy data, the interlayer Cl^- is partially substituted by OH^- rather than CO_3^{2-} groups. We suppose that the presence/absence of a band in the region 1400–1350 cm^{-1} in the Raman spectra of stichtite can be explained by the local distortion of triangular CO_3 groups. Stichtite and iowaite occur here in polytypic modifications 3*R* and 2*H* that are the most widespread for the hydrotalcite supergroup iowaite and stichtite is 2:1. For both minerals, the polytype 3*R* strongly dominates over 2*H*. The lowest 3*R*/2*H* ratio determined for the Terekta iowaite and stichtite is 2:1. The Altai stichtite is close in 3*R*/2*H* to the stichtite from Tasmania (Australia) and differs significantly from that in Transvaal samples (South Africa).

Keywords: stichtite, iowaite, woodallite, pyroaurite, hydrotalcite, layered double hydroxide, Terekta Ridge

INTRODUCTION

Stichtite $Mg_6Cr_2(OH)_{16}(CO_3)(H_2O)_4$, pyroaurite $Mg_6Fe_2^{3+}(OH)_{16}(CO_3)(H_2O)_4$, iowaite $Mg_6Fe_2^{3+}(OH)_{16}Cl_2(H_2O)_4$ and woodallite $Mg_6Cr_2(OH)_{16}Cl_2(H_2O)_4$ are members of the hydrotalcite group, which is included in the supergroup of the same name (Mills et al., 2012). Representatives of this group typically have a 3 : 1 ratio of divalent and trivalent cations $M^{2+}:M^{3+}$. In general, the minerals of the hydrotalcite supergroup belong to a large family of layered double hydroxides (LDH) that comprises natural and synthetic compounds (Rives, 2001; Evans and Slade, 2006; Mills et al., 2012).

The LDH crystal structure consists of alternating metal hydroxide layers (these are formed by octahedra, in which cations of the metal *M* are surrounded by OH groups) and a water–anion component that occupies the interlayer space (Fig. 1). In the minerals considered in this study the metal hydroxide layers have the composition $[(M^{2+}, M^{3+})(OH)_2]^+$—this is the generalized presentation we use because there are no indications of ordered positions of M^{2+} and M^{3+} cations at ratio $M^{2+}:M^{3+} = 3:1$ (Hansen and Koch, 1996; Drits and Bookin, 2001; Sideris et al., 2008). The positive charge of such layers is determined by the quantity of trivalent cations and is compensated by anions located in the interlayer space, where water molecules are also found. In our case the composition of the interlayer components corresponds to the formulae $[Cl_2(H_2O)_4]^{2-}$ for chloride and $[(CO_3)(H_2O)_4]^{2-}$ for carbonate representatives (here and thereafter the formula was calculated on the basis of Σ cation = 8 atom per formula unit, apfu). The minerals of the hydrotalcite supergroup that are most widespread in nature belong to two polytypes: *3R* (three layered rhombohedral unit cell) and *2H* (two layered hexagonal unit cell). They differ from each other in mutual position of metal hydroxide layers (Fig. 1) and are well distinguished in X-ray diffraction patterns.

The presence of a positively charged layered quasi-lattice in the crystal structure of the LDH allows using them as anion exchanging materials, which led to their widespread use in modern technologies (Li and Duan, 2006). For example, the synthetic analog of iowaite was recently proposed as a material for filtration of water contaminated by arsenic (Guo et al., 2017). Because carbonate is highly favored as an interlayer anion, and the LDHs have the ability

✉ Corresponding author.
E-mail adress: e.zhitova@spbu.ru (E.S. Zhitova)

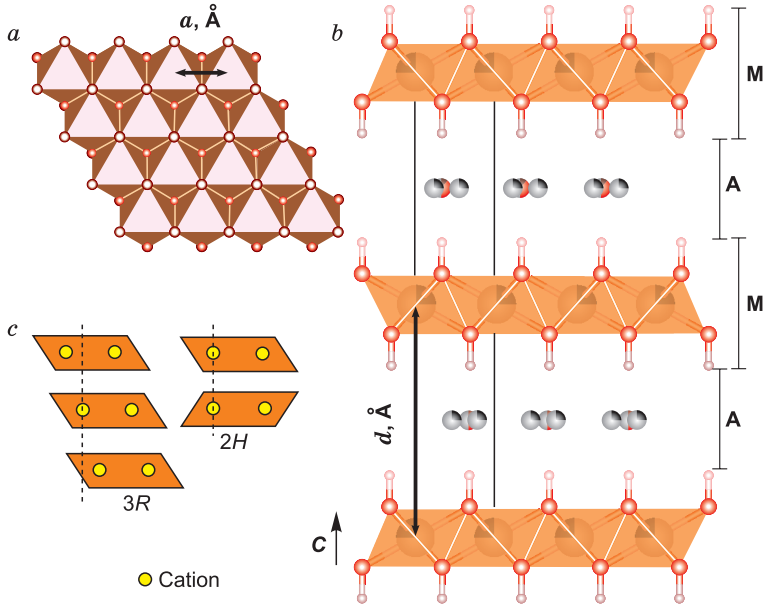

Fig. 1. Crystal structure of minerals of the hydrotalcite group: (*a*) metal hydroxide layers (projection *ab*); (*b*) alternation of metal hydroxide layers (M) and water–anion layers (A), located in the space between the *M*-layers, exemplified by a 2*H* polytype; (*c*) location of metal hydroxide layers for 3*R* polytypes (with sliding) and 2*H* polytypes (with rotation).

to "use" the CO_2 captured directly from the air during crystallization in atmospheric conditions, these compounds (including analogs of stichtite and pyroaurite) can be used for capturing atmospheric carbon dioxide in mineral form (Ram Reddy et al., 2006; Mills et al., 2011; Huang et al., 2014; Wang et al., 2016).

Most minerals of the hydrotalcite supergroup are rare and occur in small quantities. The relatively widespread members can include stichtite, which is abundant in a series of geologic setting. For example, it composes 5–20% (visual estimate) of the volume of chrysotile–lizardite serpentinites in the northern zone of the Kaznakhta ophiolite body in the Terekta Ridge of the Russian Gorny Altai (Tatarinov et al., 1985). Minerals of the hydrotalcite supergroup—stichtite, iowaite, woodallite, hydrotalcite, pyroaurite and mountkeithite—together constitute approximately 20 wt.% of the serpentinized dunite of Mount Keith (Western Australia) (Grguric, 2003; Grguric et al., 2006; Mills et al., 2011).

Stichtite is considered a mineral that forms exclusively in serpentinites of ophiolites and greenschist belts characterized by high Cr content. Here it often forms an isomorphic series with pyroaurite (Ashwal and Cairncross, 1997). Recent isotope research of stichtite from occurrences in Western Tasmania (Australia) and Tehuitzingo (Mexico) demonstrated that the formation of the mineral took place during the serpentinization of ultrabasic rocks from island arc complexes due to the action of methane- or hydrogen-enriched fluid (Melchiorre et al., 2017). At the same time, the degree of replacement of chromite by stichtite is determined by the length of the so-called "stichtite window"—the period when such a chemistry of the serpentinization process is supplemented by particular physical conditions: temperature of 300 °C and a pressure no higher than 0.8–1.2 GPa (Melchiorre et al., 2017). Specifically, for the Tasmania and Tehuitzingo material it was determined that the increased iron content in stichtite indicates a lower serpentinization temperature, and that the 2*H* polytype is a more high-temperature or high-pressure modification than the 3*R* polytype (Melchiorre et al., 2017). Note that the latter is in accord with our data for the formation conditions of various polytypes of quintinite—the Mg–Al–CO_3 member of the hydrotalcite supergroup with Mg : Al = 2 : 1 (Zhitova et al., 2018).

Stichtite mineralization in Terekta Ridge serpentinites was for the first time described in publications by Tatarinov et al. (1985). A crystallographic study of stichtite from this location (Bookin et al., 1993) showed that it is represented by 3*R* and 2*H* polytypes that are ordinary for LDHs, and an atypical 1*H* polytype that is characterized by a reduced distance between the layers. This will be discussed in more detail below.

The stichtite samples that were studied in the two papers mentioned above originate from the Kara-Uyuk River valley. Recently, in the valley of Kyzyl-Uyuk Creek a larger occurrence of stichtite was identified in similar geologic settings, containing significant amount of chrome-enriched representatives of the hydrotalcite group, that fairly varied in composition. The aim of this paper is to present the crystal chemical characteristic of these minerals, including studies of the cation and anion isomorphism, determination of common structural characteristics and of the peculiarities of H- and C-containing groups.

GEOLOGIC LOCATION OF THE MINERALIZATION AND BRIEF DESCRIPTION OF THE STUDIED MATERIALS

Occurrences of chromous minerals from the hydrotalcite group in the Kaznakhta ophiolite zone of the Terekta Ridge (northern branch of the Terekta ophiolite belt, Gorny Altai) are associating with the thrust-sheet zone of the steep Charysh–Terekta deep fault. The northern zone of the Kaznakhta ophiolite body is composed of chrysotile-lizardite serpentinites. The age of the serpentinites was determined as Carboniferous, and for some bodies it is presumably Cambrian. According to views on the tectonics of the Terekta Ridge region, in the early Cambrian and Carboniferous this was an area of complex subduction and collisional processes (Tatarinov et al., 1985; Buslov et al., 2001, 2013; Ota et al., 2007; Buslov, 2011).

The material of this study was collected in the valleys of creeks Kara-Uyuk and Kyzyl-Uyuk by V.S. Lednev in 2010 and 2011. In the Kara-Uyuk samples, like in previous studies (Tatarinov et al., 1985), we identified only stichtite. Samples from the Kyzyl-Uyuk occurrence turned out to be quite varied in composition with identified stichtite, pyroaurite, iowaite, and woodallite, which demonstrate a noticeable diversity of chemical composition. The main attention of this study was focused on material from this occurrence.

Chromous minerals of the hydrotalcite group associating in both occurrences with linear zones in the serpentinites and sometimes extending to tens of meters, are represented by massive thinly laminated aggregates of various shades of purple: from light pink-purple to bright deep violet-purple. They compose lenses and knots up to 30 cm across, as well as veinlets in the chrysotile–lizardite serpentinites (according to V.S. Lednev). Usually the chloride minerals—iowaite and woodallite—are more intensely colored in comparison to carbonate ones. This is especially clear in samples where stichtite and iowaite aggregates are intergrown: the color margin between them is always abrupt, and the former has a weaker coloring. Aggregates of studied minerals contain ingrowths of lizardite (Fig. 2).

METHODOLOGY OF RESEARCH

Electron microprobe analysis. The study of the chemical composition of the minerals was performed:

– in the "Geomodel" resource center of SPbU using a Jeol 5900LV scanning electron microscope fitted with a INCA Energy 350 energy-dispersive spectrometer (U = 20 kW, I = 2.0 nA, analyzer diameter 5–10 μm). Standard samples: MgO (Mg), Al_2O_3 (Al), Cr (Cr), FeS_2 (Fe), NaCl (Cl).

– in the Laboratory of Local Matter Investigation Methods of the Section of Petrology at MSU using a Jeol JSM-6480LV scanning electron microscope, fitted with a INCA Energy 350 energy-dispersive spectrometer (ATW-2 window, U = 20 kW, I = 1.0 nA, analyzer diameter 5 μm). Standard samples: diopside (Mg), Al_2O_3 (Al), Cr (Cr), FeAsS (Fe), ZnS (S), NaCl (Cl).

In both cases, the study was performed on polished samples coated with carbon.

Vibrational spectroscopy. The infrared (IR) spectra of mineral powders compressed in tablets with KBr were obtained on an ALPHA FTIR Fourier transform spectrometer (Bruker Optics, Germany) in the range of wave numbers 360–3800 cm^{-1} with a resolution of 4 cm^{-1} via 16 scans. The reference sample was a similar tablet made of pure KBr. Raman spectra were obtained using a Horiba Jobin-Yvon LabRam HR800 spectrometer using an ion argon laser (λ = 514.5 nm) with maximum power of 50 mW, and on-sample power 8 mW. The instrument is fitted with a microscope with a 50x magnification. The spectra were registered in the range of 70–4000 cm^{-1} with a resolution of 3 cm^{-1}. The recording of a Raman spectra was done from a grain on the slide (without preliminary orientation).

X-ray diffraction methods. Powder diffraction patterns were obtained using a single-crystal Rigaku Raxis Rapid II

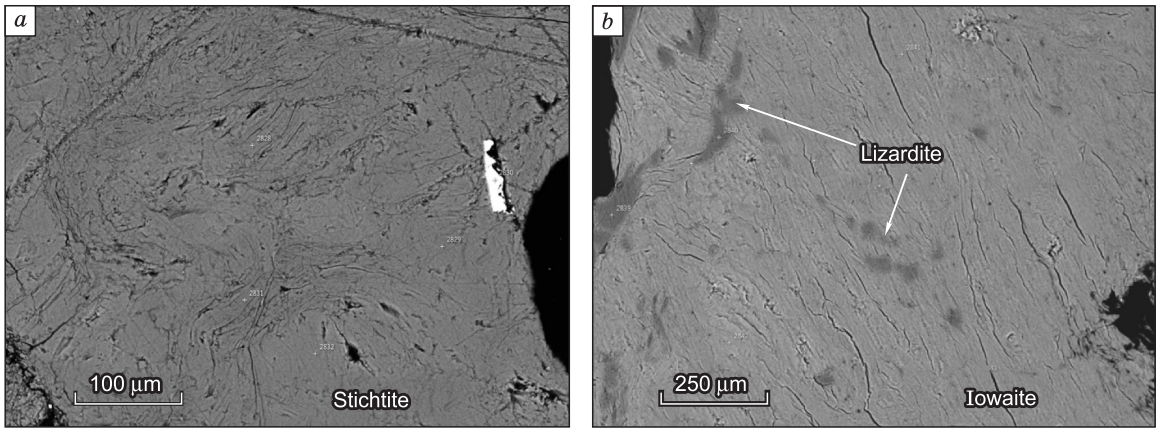

Fig. 2. Aggregates of stichtite (*a*) and iowaite (*b*) in polished sections, imaged in backscattered electrons.

diffractometer (Debye-Scherrer geometry, 127.4 mm, CoK_α radiation), equipped with a cylindrical image plate detector and a high-energy source of X-ray radiation with a rotating anode. Samples were fixed on a holder using paratone oil and centered, after which data was accumulated with rotation along the φ axis during 600 s. The files obtained were converted into standard formats that were used for processing of the powder diffraction patterns by means of osc2xrd software (Britvin et al., 2017). The X-ray patterns were obtained from three different fragments of each sample in order to average the data.

In addition, for each sample a powder pattern was recorded for a larger amount of material using a Bruker D2 Phaser powder diffractometer (Bragg-Brentano geometry, radius 140 mm, CoK_α radiation). The sample was powdered and fixed on a silica mount using Vaseline in order to reduce the texturing effect.

RESULTS

Electron microprobe analysis. Typical analyses that representatively reflect the chemical composition variations in the hydrotalcite group minerals from occurrences of the Terekta Ridge are given in Table 1. Empirical formulae were calculated for the sum of metal cations Mg + Al + Fe + Cr equal to 8 atom per formula unit, apfu. Iron valence was not determined. For analyses with Mg ≥ 6.00 apfu all iron was accepted as trivalent in accordance with results of wet chemical analyses of Terekta stichtite presented by Tatarinov et al. (1985), as well as with general crystal chemical characteristics of the members of the hydrotalcite group (Mills et al., 2012, 2016). In analyses with Mg < 6.00 apfu, formulae calculations assumed that this lack of magnesium is compensated by iron (Mg + Fe^{2+} = 6.00 apfu for analyses, where the total charge of M^{2+} cations is not below +18.00 or Mg + Fe^{2+} + Fe^{3+} = 6.00 apfu if it is less than that: the latter is dictated by the crystal chemical necessity of the presence of 16 OH groups per formula in the metal hydroxide layers) the corresponding part of the iron was accepted as divalent. The calculation of the anion part of the formulae is somewhat complicated by the presence of three components at once that are not detectable by electron microprobe analyses: two charged (CO_3^{2-}, OH^-) and one neutral (H_2O^0). The quantities of OH groups in the metal hydroxide layers and

Table 1. Chemical composition of the minerals of the system stichtite (1–4)–pyroaurite (5)–iowaite (6–10)–woodallite (11) from the manifestations of the Terekta Ridge

Component	Sample number										
	1	2	3	4	5	6	7	8	9	10	11
	3419	3418	3417a	3416	3413	3413-1	3412	3412b	10897	3412b	3412a
MgO, wt.%	38.65	35.94	37.99	36.77	38.21	34.48	37.48	36.95	38.06	36.29	35.36
Al_2O_3	5.92	1.42	2.14	2.26	1.31	1.58	2.14	1.97	2.01	1.30	1.26
Cr_2O_3	13.69	21.25	11.43	9.94	9.30	8.70	8.99	9.68	9.16	10.07	10.61
Fe_2O_3*	1.95	2.93	8.94	10.26	11.76	16.12	10.97	11.06	10.45	10.68	11.77
SO_3	b.d.l.	b.d.l.	0.05	b.d.l.	0.16	b.d.l.	b.d.l.	b.d.l.	b.d.l.	0.32	0.25
Cl	b.d.l.	b.d.l.	0.03	b.d.l.	0.11	5.85	8.62	7.70	9.97	9.44	10.55
CO_2 cal.	7.04	6.80	6.67	6.69	6.68	–	–	–	–	–	–
H_2O cal.	34.58	33.37	33.65	32.84	33.62	33.69	33.65	33.65	33.63	32.35	31.89
$–O=Cl_2$	–	–	–0.01	–	–0.02	–1.32	–1.94	–1.74	–2.25	–2.13	–2.38
Total	101.83	101.71	100.89	98.76	101.13	99.10	99.91	99.61	101.03	98.32	99.31
Mg^{2+}, apfu**	5.99	5.77	6.05	6.00	6.09	5.69	6.06	6.01	6.11	6.04	5.90
Fe^{2+}	0.01	0.23	–	–	–	0.31	–	–	–	–	0.04
Al^{3+}	0.73	0.18	0.27	0.29	0.17	0.21	0.27	0.25	0.26	0.17	0.17
Cr3+	1.13	1.81	0.96	0.86	0.79	0.76	0.77	0.83	0.78	0.89	0.94
Fe^{3+}	0.15	0.01	0.72	0.85	0.95	1.03	0.90	0.91	0.85	0.90	0.95
Cl^-	–	–	0.01	–	0.02	1.10	1.58	1.42	1.82	1.79	2.00
SO_4^{2-}	–	–	0.00	–	0.01	–	–	0.03	–	0.03	0.02
CO_3^{2-}	1.00	1.00	0.98	1.00	0.975	–	–	–	–	–	–
OH^-***	16	16	16	16	16	16.90	16.36	16.51	16.18	16.11	16.00
H_2O^0	4	4	4	4	4	4	4	4	4	4	4

Note. 1, Kara-Uyuk River valley; 2–11, Kyzyl-Uyuk River valley. Values for CO_2 and H_2O–calculated; b.d.l., below detection limit of electron microprobe analysis.

* All iron in this part of the table is represented as trivalent for simplicity.

** Calculated on the basis of Mg + Al + Fe + Cr = 8.

*** Number of OH-groups, relating to the metal hydroxide layers is 16.00; analyses 6–10 have additional OH-groups, located in the interlayer space and compensating the lack of chlorine (explanations in text).

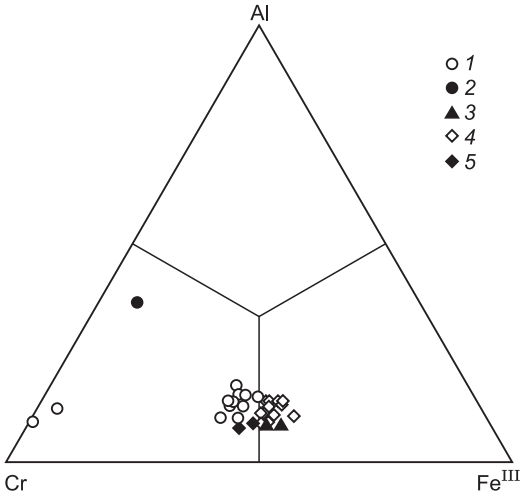

Fig. 3. Atomic ratios of trivalent cations (comments on formulae calculations in the text) in the studied minerals of the hydrotalcite group from the Terekta Ridge occurrences: *1,* stichtite, Kyzyl-Uyuk; *2*, stichtite, Kara-Uyuk; *3*, pyroaurite, *4*, iowaite, *5*, woodallite (all Kyzyl-Uyuk).

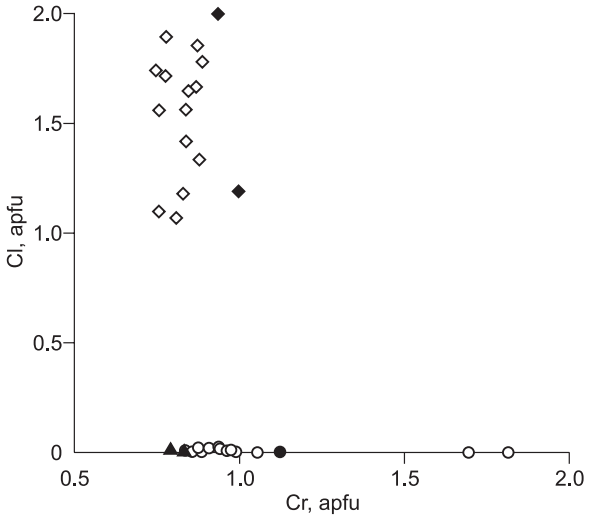

Fig. 4. Relationship between chromium and chlorine in the studied minerals of the hydrotalcite group from the Terekta Ridge occurrences. See Fig. 3 for designations.

H_2O molecules of the interlayer space are in both cases accepted as equal to 16 and 4 apfu correspondingly, in accordance with the stoichiometry of these minerals. In carbonate-bearing minerals: stichtite and pyroaurite—the balancing of charges was done by variation of the number of CO_3 groups. In significantly chlorine-bearing minerals—iowaite and woodallite—the CO_3 groups content can be null or negligible (judging from IR spectroscopy data see below), and the balancing of charges was in this case done by variation of the number of OH groups: it is assumed that OH^- replaces Cl^- in the interlayer space.

Divalent cations in minerals of both occurrences are nearly exclusively represented by magnesium. Only in rare cases its content does not reach 6 apfu, and even in these cases the deficit is slight: no more than 0.31 apfu (Table 1, an. 6), which is only 5 rel.% of the total Mg^{2+}. On the contrary, ratios of trivalent cations vary quite widely, especially the Fe : Cr value. These variations are shown on Fig. 3. Regarding Cl concentration samples can be clearly divided into two groups: Cl-poor species (having <0.2 wt.%, i.e., 0.01 apfu of Cl) and Cl-rich (having 5.8–10.6 wt.%, i.e., 1.1–2.0 apfu of Cl) (Table 1, Fig. 4).

Vibrational spectroscopy. Infrared and Raman spectra of hydrotalcite group minerals from the Terekta Ridge serpentinites are shown on Figs 5–7. For comparison, Fig. 6 shows IR spectra of iowaite samples with high Fe^{3+} contents from the Korshunovskoe iron ore deposit in the Irkutsk oblast (light green veinlets cutting dolomite marble) and from the Talnakh copper-nickel deposit in the Krasnoyarsk Territory (pale-yellow tabular crystals ingrown in gypsum).

Bands observed in the IR spectra in the range 3300–3700 cm^{-1} are due to O–H-stretching vibrations. Even though in hydrotalcite group minerals the hydroxyl groups belong to the brucite-like layer, their state is radically different from that in brucite. The latter's IR spectrum contain a single narrow band close to 3700 cm^{-1} in the area of the O–H-stretching vibrations, which indicates a very low strength of the hydrogen bond (effectively a lack of the bond). The strongest hydrogen bonds are formed by OH groups in the highly aluminous stichtite (smp. 3419), as well as some OH groups in the minerals of the woodallite-iowaite series. Similar bands of O–H-stretching vibrations are present in the IR spectra of stichtite and iowaite (Fig. 7).

The intensive shoulder at 3000–3080 cm^{-1} observed in the IR spectra of some samples (Fig. 5) corresponds to weakly acid OH-bearing groups. In the IR spectrum for smp. 3419, where this shoulder is the most distinct, there is also a very weak band at 1735 cm^{-1}. Together these facts allow us to infer the existence of a small admixture of the Zundel cation (that is, the hydrated proton $H_5O_2^+$) (Chukanov and Chervonnyi, 2016) in the stichtite-pyroaurite series minerals.

Bands in the 1630–1660 cm^{-1} range correspond to bending vibrations of water molecules. The frequency of this band characteristically increases with the increase of carbonate groups in the mineral.

Bands in the 1360–1390 cm^{-1} range correspond to stretching vibrations of the CO_3^{2-} group. In the IR spectrum of the Cl-depleted iowaite (Fig. 6; smp. 3413-1—curve *3*) this band has a low intensity, from which we can conclude that the chlorine deficit is replenished by mainly OH groups and to a much lesser extent by CO_3^{2-} groups.

The IR spectrum for iowaite from the Talnakhskoe deposit has an interesting feature in the presence of weak, relatively narrow bands at 1402 and 1284 cm^{-1}. The last band can only possibly be attributed to BO_3^{3-} groups. The presence of doublet bands in the 1260–1410 cm^{-1} range of the

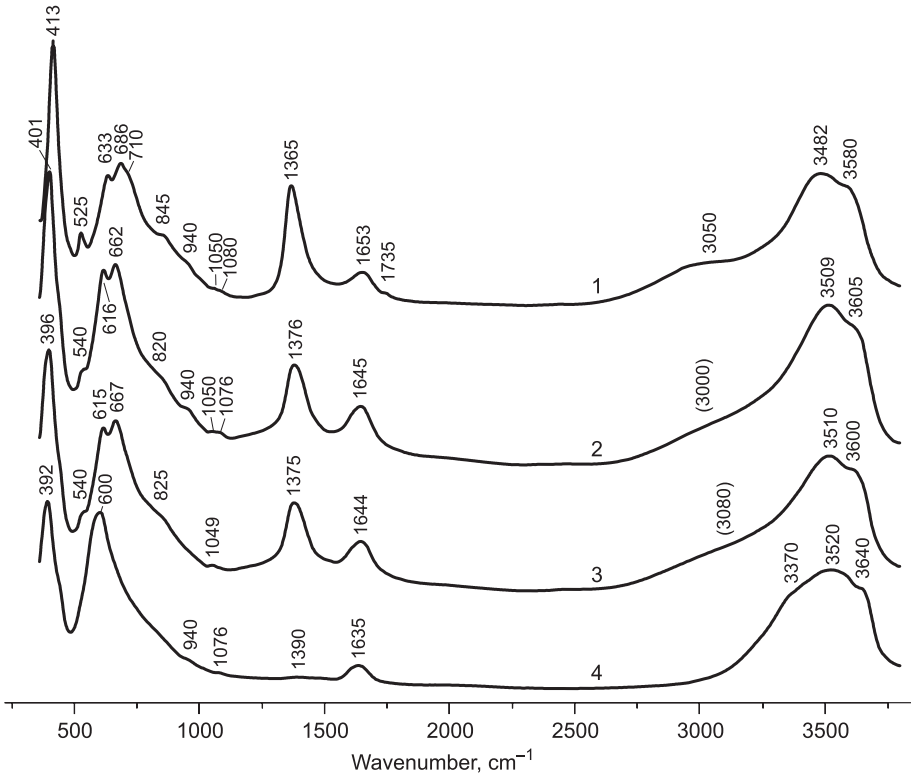

Fig. 5. IR spectra of high-aluminiferous stichtite, smp. 3419 (1), Fe^{3+}-rich stichtite, smp. 3417 (2), Cr^{3+}-rich pyroaurite, smp. 3413 (3), and an intermediate member of the iowaite-woodallite series, smp. 3412 (4).

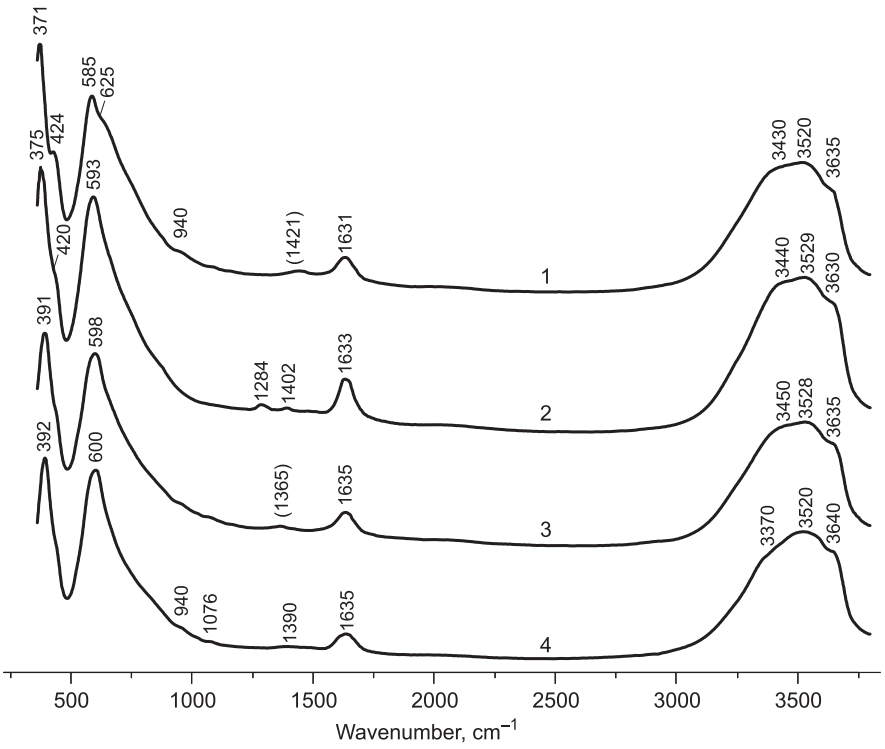

Fig. 6. IR spectra of iowaite of the composition $Mg_{5.87}Fe_{2.04}Al_{0.09}(OH)_{16}Cl_{1.87}(OH)_{0.13}\cdot nH_2O$ from the Korshunovskoe deposit, Irkutsk oblast (1), iowaite of the composition $Mg_{6.01}Fe_{1.67}Al_{0.31}Cr_{0.01}(OH)_{16}Cl_{1.87}(OH,BO_3)_x\cdot nH_2O$ from the Talnakhskoe deposit, Krasnoyarsk Territory (2), Cr-enriched Cl-depleted iowaite, smp. 3413-1 (3), and an intermediate member of the iowaite-woodallite series, smp. 3412 (4).

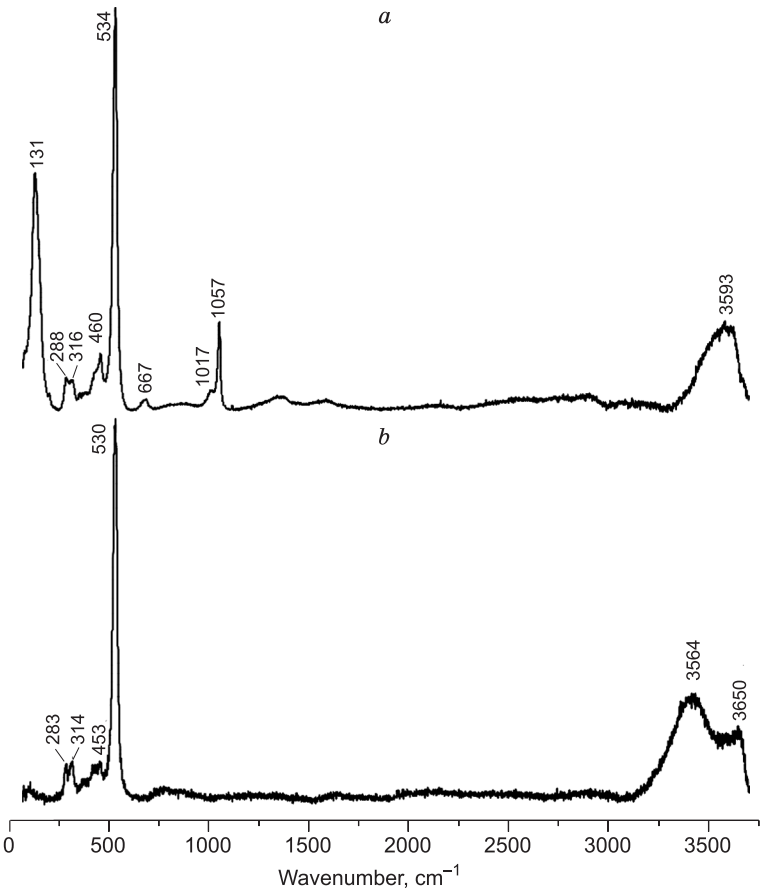

Fig. 7. Raman spectra for: *a*, stichtite, smp. 3416; *b*, iowaite, smp. 10897.

IR spectrum is typical for a strongly distorted BO_3 triangle (Chukanov et al., 2018).

Very weak bands in the range of 900–1100 cm^{-1} of the IR spectra most probably correspond to mechanical admixtures, including lizardite (bands at 940 cm^{-1} and possibly ~1076 cm^{-1}). Local bending vibrations of $M\cdots$O–H and CO_3^{2-}, as well as $M^{3+}\cdots$O stretching vibrations should have appeared in the range 450–900 cm^{-1} in the form of a series of narrow bands. Instead, in the IR spectra of the hydrotalcite group minerals there are wide, badly resolved bands in the middle part of this range. Thus, instead of local vibrations of these types there are mixed lattice modes with changing angles of $M\cdots$O–H and O–C–O and bond lengths of $M^{3+}\cdots$O.

A narrower band in the 371–413 cm^{-1} range is mostly related to $M\cdots$O stretching vibrations. With the increase of the average mass of the *M*-cation its position shifts towards the low frequencies area.

A typical feature of the Raman spectrum of stichtite that differentiates it from the iowaite spectrum is the presence of bands in the 1010–1060 cm^{-1} area, corresponding to symmetrical stretching vibrations of carbonate groups (Fig. 7).

When comparing the stichtite IR spectrum with published data there arises the problem of interpretation of the Raman band at 1350–1400 cm^{-1}, which is forbidden for the symmetrical CO_3^{2-} group. It corresponds to asymmetrical C–O-stretching vibrations and is not always present in carbonate LDH spectra. The Raman band in the 1350–1400 cm^{-1} range was recorded for stichtite of Tasmania (Mills et al., 2011), but was found neither in the stichtite spectrum of Terekta Ridge nor during studies of synthetic analogs of stichtite (Frost and Erickson, 2004). The appearance of this band was attributed to an admixture of the 2*H* polytype (Mills et al., 2011). However, recent studies of pyroaurite-*3R* (Zhitova et al., 2016) in which the 2*H* polytype admixture was not found, showed a Raman band at 1346 cm^{-1}. Based on this, we assume that the changeable character of the absorption band's appearance between 1350 and 1400 cm^{-1} in Raman spectra of carbonate LDHs can be due to local situations, leading to distortions of the CO_3 triangle.

Intense bands with wave numbers at 534 and 530 cm^{-1} in stichtite and iowaite IR spectra are very close in position and intensity and are attributed by us to lattice modes, in particular to symmetrical vibrations of bonds in Mg–O–Mg (Mora et al., 2014), and not to carbonate groups, as was proposed in several previous publications (Frost and Erickson, 2004; Theiss et al., 2013).

X-ray powder diffraction. Powder diffraction patterns of the studied samples are given in Fig. 8. In addition to reflections of hydrotalcite-group minerals, some patterns dis-

Table 2. Main crystal chemical characteristics of the studied samples

Sample	Fragment	a^*, Å[(1)]	d, Å[(2)]	3*R*/2*H*/lizardite[(3)], (= 3*R*/2*H*)	3*R*/2*H*[(4)]
Stichtite					
3416 (an. 4 in Table 1)	1 D-S[(5)]	3.10	7.85	61/39 = 2/1	2/1
	2 D-S	3.10	7.85	76/24 = 3/1	4/1
	3 D-S	3.10	7.84	77/23 = 3/1	3/1
	4 B-B	–	7.90	–	3/1
94743	1 D-S	3.09	7.78	75/20/5 = 4/1	3/1
	2 D-S	3.08	7.76	72/24/4 = 3/1	3/1
	3 D-S	3.09	7.78	77/14/9 = 6/1	7/1
	4 B-B	–	7.78	–	–[(6)]
Iowaite					
10897 (an. 9 in Table 1)	1 D-S	3.10	8.01	–	5/1
	2 D-S	3.11	8.04	–	7/1
	3 D-S	3.11	8.04	–	7/1
	4 B-B	–	8.04	–	5/1

Note. [(1)] calculated for $d_{110} \times 2$, [(2)] the c parameter can be calculated for $d_{00n} \times 3$ (for the 3*R* polytype) or $d_{00n} \times 2$ (for the 2*H* polytype), [(3)] calculated by Rietveld refinement using Topas software (Bruker, 2009); [(4)] calculated from reflexes ratio *015*(3*R*)/*103*(2*H*); [(5)] 1, 2, 3 and 4, grain number; D–S, Debye-Scherrer geometry; B-B, Bragg-Brentano geometry; [(6)] not calculated due to very low intensity of nonbase reflexes; dash, not calculated.

play weak reflections of lizardite, which was found in close association with them (Fig. 2).

Stichtite and iowaite from the Kyzyl-Uyuk occurrence were studied in the most detail using this method. They demonstrate two polytypes: 3*R* and 2*H* that are typical for hydrotalcite group minerals. To characterize the unit cell sizes, we used the interlayer distance (d_{00n}), that is the shortest distance between two metal hydroxide layers, and the a^* parameter—the distance between two closest *M*-cations located in adjacent octahedrons of a single layer. For crystal structures characterized by various disorderly distributed of cations in the metal hydroxide layers, the a^* parameter is equivalent to the a parameter of the unit cell (like in our case) (Fig. 1). For polytypes that have a superstructure in the plane of the metal hydroxide layers, a^* is the subunit parameter. Parameters d and a^* are given in Table 2. Carbonate and chlorine representatives of the hydrotalcite group differentiate well by the value of the interlayer distance (d_{00n}), which is ~7.8 Å for the former (hydrotalcite, pyroaurite (Zhitova et al., 2016)) and ~8.0 Å for the latter (for example, 8.04 Å for iowaite (Braithwaite et al., 1994)). Interlayer distance values close to these were obtained for our samples as well (Table 2).

The ratio of *3R/2H* polytypes (Table 2) for our samples was calculated by two methods: (1) based on results obtained by the Rietveld method (only for stichtite) using the Topas software (Bruker, 2009), and (2) according to the ratio of 015(3*R*)/013(2*H*) reflection intensities (Fig. 9). For structural models used in Rietveld method calculations of stichtite polytype ratios we used data for hydrotalcite-*3R* and hydrotalcite-2*H* (analogs of existing stichtite modifications, but with Al instead of Cr) that were obtained previously using single-crystal X-ray diffraction (Zhitova, 2019). Because the structural model for iowaite-*2H* is unknown, we did not do a Rietveld refinement for our iowaite, and the 3*R/2H* ratio was estimated only using the second method. Since for stichtite the determination of polytype ratios was done using both methods (Table 2), it was possible to estimate the deviations in the determination of the 3*R/2H* ratio by different methods which appeared to be ≤ 5%. For example, for smp. 3416 2 D-S (Table 2) the 3*R/2H* ratio determined by the first method 76/24, and the one determined by the second: 4/1 (80/20), meaning the deviation in values determined by different methods is 4%.

DISCUSSION OF RESULTS

Chemical composition and its variations. As can be seen on Table 1 and Figs. 3, 4, four minerals of the hydrotalcite group forming a solid solution system were identified in the Kyzyl-Uyuk occurrence. Two separate series can be isolated according to the ratio of additional anions: the carbonate series that includes stichtite and the Cr^{3+}-rich pyroaurite; and the chloride species that comprises highly ferrous iowaite and woodallite. Note that the finding of woodallite is the first for Russia. These series are very clearly differentiated by the interlayer anion: carbonate minerals are nearly depleted in chlorine, and chloride ones in carbonate groups. This is clearly indicated by electron microprobe (for Cl) and IR spectroscopy (for CO_3) data. The existence of this differentiation is also starkly illustrated by the fact that iowaite and stichtite aggregates when together always have an abrupt boundary, notably without evidence of replacement

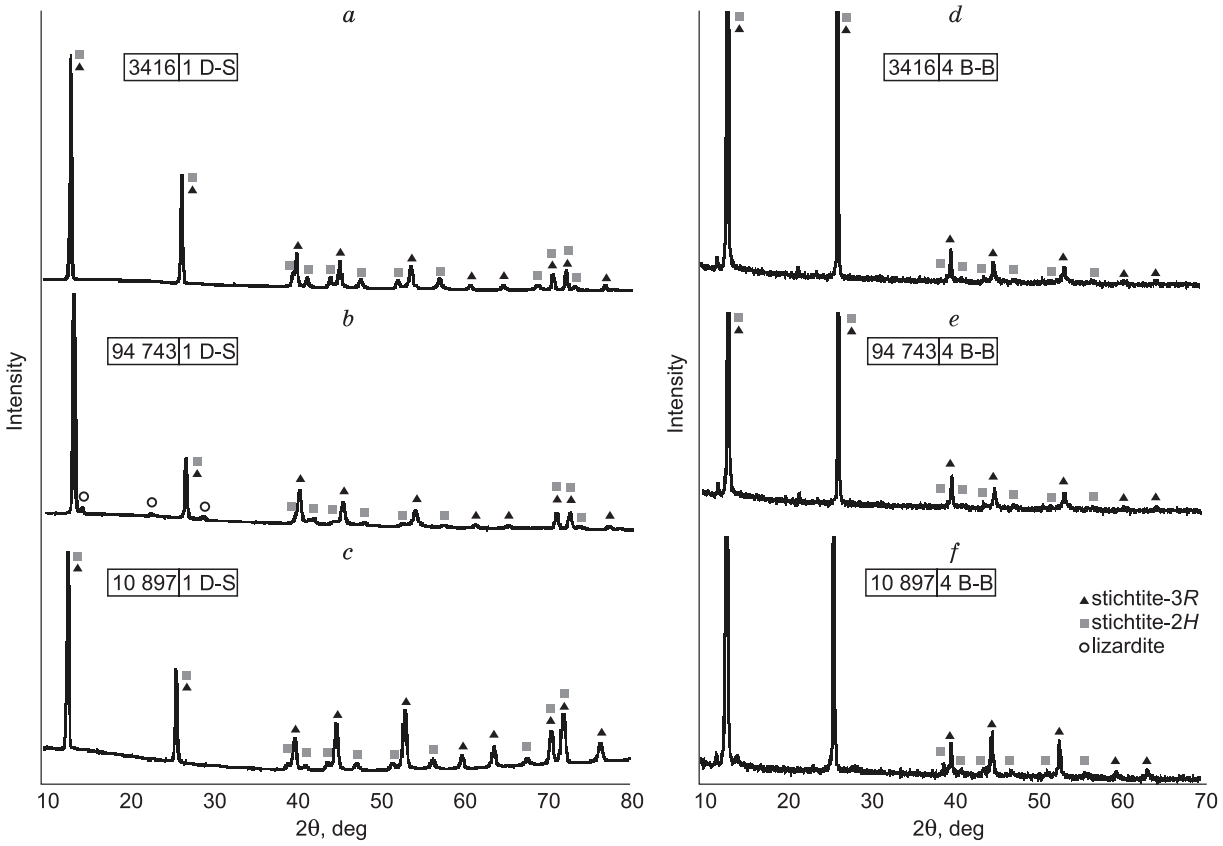

Fig. 8. X-ray powder diffraction pattern of the studied samples, CoK_α radiation. *a–c*, Debye-Scherrer geometry; *d–f*, Bragg-Brentano geometry, first basal reflex is cut off at relative intensity values of ~20%.

of one mineral by the other. So, we can assume with high probability that iowaite and stichtite crystallized together in such aggregates. This indicates that the nearly complete division of interlayer Cl^- and CO_3^{2-} anions between the phases was caused by their crystal chemical differences, as opposed to some geochemical or other external cause.

The chlorine content in minerals of the iowaite-woodallite series varies significantly: from 1.1 to 2.0 at.% (Table 1, Fig. 4). At the same time, the IR spectra of the samples with different Cl content are close: the "chlorine-lacking" iowaite also lacks CO_3 groups absorption bands of at least some intensity, which is the same for the "fully-Cl" iowaite (Figs. 5, 6). It is probable, that there is an $OH^- \rightarrow Cl^-$ replacement in the interlayer space. Results of detailed studies of iowaite (including quantitative determination of carbon) from the alkaline-ultrabasic Palabora pluton (South Africa) (Braithwaite et al., 1994) yielded its empirical formula as such: $(Mg_{5.9}Fe^{2+}_{0.1}(OH)_{16}[Cl_{1.40}(OH)_{0.48}(CO_3)_{0.06}](H_2O)_4$.Thus, here is also a replacement of Cl^- by mainly OH^- rather than by CO_3^{2-}. The possibility of such a replacement is also indirectly confirmed by the existence of minerals, in which the interlayer anions are represented only by hydroxyl groups, for

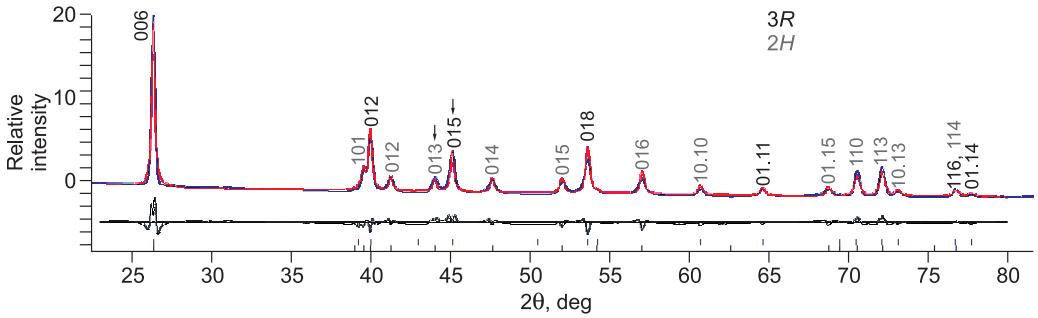

Fig. 9. Comparison of experimental and calculated X-ray pattern of stichtite (smp. 3416-1). Arrows show reflections, whose relative intensity values were used to estimate 3*R*/2*H*.

example meixnerite $Mg_6Al_2(OH)_{16}(OH)_2 \cdot 4H_2O$ (Koritnig and Süsse, 1975). One should note that Frost et al. (2005) have determined that the synthetic analog of iowaite "oxidizes" in open air with replacement of Cl^- by CO_3^{2-} [1]. Our work has not yielded any evidence for such a replacement for iowaite and woodallite. The lack of replacement of chlorine with carbonate is confirmed by existing samples with full and almost full occupancy of the interlayer space with chlorine (Table 1), although they were stored in the open air for several years.

The second factor causing the diversity of the hydrotalcite group minerals of the Kyzyl-Uyuk occurrence is the isomorphism of the M^{3+} cations. As is shown on Fig. 3, most analyses on the Cr–Fe^{3+}–Al diagram are clustered around the line of equal Cr and Fe content, which means we are observing Fe^{3+}-rich variations of stichtite and woodallite, transitioning to Cr^{3+}-rich variations of pyroaurite and iowaite respectively. The content of Cr_2O_3 in minerals that correspond to this rather compact composition field varies between 8.7 and 11.4 wt.%. In addition, on Kyzyl-Uyuk there was found a Cr-enriched (up to 21.3 wt.% of Cr_2O_3) and Fe-depleted stichtite (Table 1, an. 2). The Al_2O_3 content in all minerals of this occurrence is low: from 1.3 to 2.3 wt.%.

Stichtite from Kara-Uyuk is noticeably enriched in Al (~6 wt.% on average) and depleted in iron in comparison to the Kyzyl-Uyuk occurrence minerals (Table 1, an. 1).

Particularities of the crystal structure. X-ray patterns of the Terekta stichtite and iowaite show reflections typical for 3*R* and 2*H* LDH polytypes, and the other reflections correspond to lizardite. Thus, we have not found stichtite-1*H* in our Kyzyl-Uyuk material. We remind that its existence was indicated in the study by Bookin et al. (1993), who supposed that it appears from changes in "ordinary" stichtite under sunlight or X-ray irradiation, together with changing its color from purple to green. The 1*H* modification described by the authors was characterized by a reduction of the interlayer distance by 0.4 Å as compared to "normal" stichtite (that is from 7.8 to 7.4 Å). However, a later study by Hansen and Koch (1996) indicated that the reflection attributed by Bookin et al. (1993) to stichtite-1*H* could actually correspond to a chlorite impurity. We came to a similar conclusion: stichtite (including from Terekta) does not change under sunlight or X-rays, and the reflection determined by Bookin et al. (1993) as stichtite-1*H* actually correspond to a mechanical admixture of lizardite (which is indeed green in this case). In addition, note that it is hard to assume such a strong reduction of the interlayer distance (by 0.4 Å) without a significant change in the chemical composition of stichtite. Correspondingly, this hypothetical "1*H* modification" would not be called stichtite, even if it was a product of some transformation of this mineral that probably require changes in mineral chemistry.

[1] Author's note: it is unclear in the cited study, where does the chlorine go.

It is interesting that in addition to typical reflection of the 3*R* polytype (Allmann and Donnay, 1969; Braithwaite et al., 1994) the X-ray patterns for the Terekta iowaite display distinct reflection of the 2*H* modification. As far as we know, it is the first indication that iowaite has a 2*H* polytype in addition to *3R*.

Supposing the formation of LDH polytypes is determined by thermodynamic conditions (Allmann, 1968; Pausch et al., 1986; Melchiorre et al., 2017; Zhitova et al., 2018), it is logical to conclude that the 3*R*/2*H* polytypes ratio can be an indicator characteristic that can allow estimating formation conditions for minerals of the hydrotalcite supergroup. In our case, it could indicate the serpentinization conditions (Melchiorre et al., 2017). Earlier, the 3*R*/2*H* polytype ratio was determined for stichtite from the Dundas Region (Western Tasmania, Australia) and from Kaapsehoop (Transvaal, South Africa) (Mills et al., 2011). For the Terekta samples, we established that the 3*R* polytype prevails strongly over 2*H* in all cases: the lowest 3*R*/2*H* ratio is 2/1. Thus, by polytype ratio the stichtite samples of the Terekta Ridge are close to those from Tasmania, in which 3*R*/2*H* = 4/1, while the samples from Kaapsehoop differ strongly from the Terekta and Tasmania material by their high *2H* polytype content: 3*R*/2*H* = 55/45 and 46/54 (Mills et al., 2011).

We are grateful to V.S. Lednev for providing samples for studies and information on the conditions of findings of the hydrotalcite group minerals on the Kyzyl-Uyuk occurrence. This research was performed in resource centers of SPBU "X-ray diffraction investigation methods" and "Geomodel" by specialists, to whom we also express our thanks.

This study was supported by a grant of the Russian Science Foundation (No. 17-77-10023).

REFERENCES

Allmann, R., 1968. The crystal structure of pyroaurite. Acta Crystallogr. B24, 972–977.

Allmann, R., Donnay, J.D.H., 1969. About the structure of iowaite. Am. Mineral. 54, 296–299.

Ashwal, L.D., Cairncross, B., 1997. Mineralogy and origin of stichtite in chromite-bearing serpentinites. Contrib. Mineral. Petrol. 127, 75–86.

Bookin, A.S., Cherkashin, V.I., Drits, V.A., 1993. Reinterpretation of the X-ray diffraction patterns of stichtite and reevesite. Clays Clay Miner. 41, 631–634.

Braithwaite, R.S.W., Dunn, P.J., Pritchard, R.G., Paar, W.H., 1994. Iowaite, a re-investigation. Mineral. Mag. 58, 79–85.

Britvin, S.N., Dolivo-Dobrovolskii, D.V., Krzhizhanovskaya, M.G., 2017. Software for processing X-ray powder data obtained from a Rigaku RAXIS RAPID II cylinder diffractometer. Zap. RMO 146 (3), 104–107.

Bruker, A.X.S., 2009. Topas V4.2: General Profile and Structure Analysis Software for Powder Diffraction Data. Karlsruhe, Germany.

Buslov, M.M., 2011. Tectonics and geodynamics of the Central Asian Foldbelt: the role of Late Paleozoic large-amplitude strike-slip faults. Russian Geology and Geophysics (Geologiya i Geofizika) 52 (1), 52–71 (66–90).

Buslov, M.M., Saphonova, I.Yu., Watanabe, T., Obut, O.T., Fujiwara, Y., Iwata, K., Semakov, N.N., Sugai, Y., Smirnova, L.V., Kazansky, A.Yu.,

2001. Evolution of the Paleo-Asian Ocean (Altai–Sayan Region, Central Asia) and collision of possible Gondwana-derived terranes with the southern marginal part of the Siberian continent. Geosci. J. 5, 203–224.

Buslov, M.M., Geng, H., Travin, A.V., Otgonbaatar, D., Kulikova, A.V., Ming, Chen, Stijn, G., Semakov, N.N., Rubanova, E.S., Abildaeva, M.A., Voitishek, E.E., Trofimova, D.A., 2013. Tectonics and geodynamics of Gorny Altai and adjacent structures of the Altai–Sayan folded area. Russian Geology and Geophysics (Geologiya i Geofizika) 54 (10), 1250–1271 (1600–1627).

Chukanov, N.V., Chervonnyi, A.D., 2016. Infrared Spectroscopy of Minerals and Related Compounds. Springer, Cham.

Chukanov, N.V., Panikorovskii, T.L., Chervonnyi, A.D., 2018. Concerning the connection between crystal chemical characteristics of minerals of the vesuvian group and their IR spectra. Zapiski RMO 146 (1), 112–128.

Drits, V.A., Bookin, A.S., 2001. Crystal structure and X-ray identification of layered double hydroxides. Rives, 39–92.

Evans, D.G., Slade, R.C.T., 2006. Structural aspects of layered double hydroxides, in: Duan, X., Evans, G.E. (Eds.), Layered Doudle Hydroxides (Structure and Bonding). Springer, Berlin, Heidelberg, Vol. 119, pp. 1–88.

Frost, R.L., Erickson, K.L., 2004. Vibrational spectroscopy of stichtite. Spectrochim. Acta A 60, 3001–3005.

Frost, R.L., Adebajo, M.O., Erickson, K.L., 2005. Raman spectroscopy of synthetic and natural iowaite. Spectrochim. Acta A 61, 613–20.

Grguric, B.A., 2003. Minerals of the MKD5 nickel deposit, Mount Keith, Western Australia. Australian J. Miner. 9, 55–71.

Grguric, B.A., Rosengren, N.M., Fletcher, C.M., Hronsky, J.M.A., 2006. Type 2 deposits: geology, mineralogy and processing of the Mount Keith and Yakabindi orebodies, Western Australia. Soc. Econ. Geol. Sp. Publ. 13, 119–138.

Guo, Q., Cao, Y., Zhuang, Y., Yang, Y., Wang, M., Wang, Y., 2017. Effective treatment of arsenic-bearing water by a layered double metal hydroxide: Iowaite. Appl. Geochem. 77, 206–212.

Hansen, H.C.B., Koch, C.B., 1996. Local ordering of chromium(III) in trioctahedral hydroxide sheets of stichtite studied by ion exchange chromatography. Clay Miner. 31, 53–61.

Huang, L., Wang, J., Gao, Y., Qiao, Y., Zheng, Q., Guo, Z., Zhao, Y., O'Hare, D., Wang, Q., 2014. Synthesis of $LiAl_2$-layered double hydroxides for CO_2 capture over a wide temperature range. J. Mat. Chem. Sect. A 2, 18,454–18,462.

Koritnig, S., Süsse, P., 1975. Meixnerit, $Mg_6Al_2(OH)_{18}\cdot 4H_2O$, ein neues magnesium-aluminium-hydroxid-mineral. Tschemaks Mineralogische und Petrologische Mitteilungen 22, 79–87.

Li, F., Duan, X., 2006. Applications of layered double hydroxides, in: Duan, X., Evans, G.E. (Eds.), Layered Double Hydroxides (Structure and Bonding). Springer, Berlin, Heidelberg, Vol. 119, pp. 193–224.

Melchiorre, E.B., Bottrill, R., Huss, G.R., Lopez, A., 2017. Conditions of stichtite ($Mg_6Cr_2(OH)_{16}(CO_3)\cdot 4H_2O$) formation and its geochemical and isotope record of early Phanerozoic serpentinizing environments. Geochim. Cosmochim. Acta 197, 43–61.

Mills, S.J., Whitfield, P.S., Wilson, S.A., Woodhouse, J.N., Dipple, G.M., Raudsepp, M., Francis, C.A., 2011. The crystal structure of stichtite, re-examination of barbertonite, and the nature of polytypism in MgCr hydrotalcites. Am. Mineral. 96, 179–187.

Mills, S.J., Christy, A.G., Génin, J.-M.R., Kameda, T., Colombo, F., 2012. Nomenclature of the hydrotalcite supergroup: natural layered double hydroxides. Mineral. Mag. 76, 1289–1336.

Mills, S.J., Christy, A.G., Schmitt, R.T., 2016. The creation of neotypes for hydrotalcite. Mineral. Mag. 80, 1023–1029.

Mora, M., Jiménez-Sanchidrián, C., Ruiz, R.R., 2014. Raman spectroscopy study of layered-double hydroxides containing magnesium and trivalent metals. Mater. Lett. 120, 193–195.

Ota, T., Utsunomiya, A., Uchio, Y., Isozaki, Y., Buslov, M.M., Ishikawa, A., Maruyama, S., Kitajima, K., Kaneko, Y., Yamamoto, H., Katayama, I., 2007. Geology of the Gorny Altai subduction–accretion complex, southern Siberia: Tectonic evolution of an Ediacaran–Cambrian intra-oceanic arc-trench system. J. Asian Earth Sci. 30, 666–695.

Pausch, I., Lohse, H.-H., Schurmann, K., Allmann, R., 1986. Synthesis of disordered and Al-rich hydrotalcite-like compounds. Clays Clay Miner. 34, 507–510.

Ram Reddy, M.K., Xu, Z.P., Lu, G.Q. (Max), Diniz da Costa, J.C., 2006. Layered double hydroxides for CO_2 capture: structure evolution and regeneration. Ind. Eng. Chem. Res. 45, 22, 7504–7509.

Rives, V., 2001. Layered Double Hydroxides: Present and Future. Nova Science Publishers, Inc., New York.

Sideris, P.J., Nielsen, U.G., Gan, Z., Grey, C.P., 2008. Mg/Al ordering in layered double hydroxides revealed by multinuclear NMR spectroscopy. Science 321, 113–117.

Tatarinov, A.V., Sapozhnikov, A.N., Prokudin, S.G., Frolova, L.P., 1985. Stichtite in serpentinites of the Terekta Ridge (Gorny Altai). Zap. VMO 114, 575–580.

Theiss, F.L., Ayoko, G.A., Frost, R.L., 2013. Stichtite: a review. Clay Miner. 48, 143–148.

Wang, J., Huang, L., Zheng, Q., Qiao, Y., Wang Q., 2016. Layered double hydroxides/oxidized carbon nanotube nanocomposites for CO_2 capture. J. Ind. Eng. Chem. 36, 255–262.

Zhitova E.S., 2016. Crystal Chemistry of Natural Layered Double Hydroxides. PhD Thesis [in Russian]. SPbGU, Saint Petersburg.

Zhitova, E.S., Krivovichev, S.V., Pekov, I.V., Yakovenchuk, V.N., Pakhomovsky, Ya.A., 2016. Correlation between the *d*-value and the M^{2+} : M^{3+} cation ratio in Mg–Al–CO_3 layered double hydroxides. Appl. Clay Sci. 130, 2–11.

Zhitova, E.S., Krivovichev, S.V., Yakovenchuk, V.N., Ivanyuk, G.Yu., Pakhomovsky, Ya.A., Mikhailova, J.A., 2018. Crystal chemistry of natural layered double hydroxides. 4. Crystal structures and evolution of structural complexity of quintinite polytypes from the Kovdor alkaline massif, Kola peninsula, Russia. Mineral. Mag. 82 (2), 329–346.

Zhitova, E.S., Krivovichev, S.V., Pekov, I.V., Greenwell, H.C., 2019. Crystal chemistry of natural layered double hydroxides. 5. Single-crystal structure refinement of hydrotalcite, $[Mg_6Al_2(OH)_{16}](CO_3)(H_2O)_4$. Miner. Mag. 83 (2), 269–280.

Editorial responsibility: V.S. Shatsky